Volume 1 | Number 1 | Jan 2013 | Pages 1–100

ChemComm

Chemical Communications
www.rsc.org/chemcomm

ROYAL SOCIETY OF CHEMISTRY

This is an *Accepted Manuscript*, which has been through the Royal Society of Chemistry peer review process and has been accepted for publication.

Accepted Manuscripts are published online shortly after acceptance, before technical editing, formatting and proof reading. Using this free service, authors can make their results available to the community, in citable form, before we publish the edited article. We will replace this *Accepted Manuscript* with the edited and formatted *Advance Article* as soon as it is available.

You can find more information about *Accepted Manuscripts* in the **Information for Authors**.

Please note that technical editing may introduce minor changes to the text and/or graphics, which may alter content. The journal's standard **Terms & Conditions** and the **Ethical guidelines** still apply. In no event shall the Royal Society of Chemistry be held responsible for any errors or omissions in this *Accepted Manuscript* or any consequences arising from the use of any information it contains.

Chem. Commun.

COMMUNICATION

Mechanism of a one-photon two-electron process in photocatalytic hydrogen evolution from ascorbic acid with a cobalt chlorin complex†

Shoko Aoi,[a] Kentaro Mase,[a] Kei Ohkubo[ab] and Shunichi Fukuzumi[*abc]

A one-photon two-electron process was made possible in photocatalytic H_2 evolution from ascorbic acid with a cobalt(II) chlorin complex [Co^{II}(Ch)] via electron transfer from ascorbate to the excited state of [$Ru(bpy)_3$]$^{2+}$ followed by electron transfer from [$Ru(bpy)_3$]$^+$ to Co^{II}(Ch) with proton to give the hydride complex, which reacts with proton to produce H_2. [Co^{III}(Ch)]$^+$ was reduced by ascorbate to reproduce Co^{II}(Ch).

Photocatalytic production of hydrogen (H_2) has attracted increasing attention as a clean energy source because of the ever-increasing demand for energy and climate change on our planet.[1] A number of highly efficient hydrogen evolving systems have been developed including homogeneous and heterogeneous photocatalytic systems.[2-13] Two electrons are required to produce H_2 from protons, although one photon generates normally only one electron. A mechanism of photocatalytic production of H_2 was reported to clarify how photoinduced electron transfer of a photosensitiser (a one-electron process) leads to H_2 production (a two-electron process).[14-16] Disproportionation of one-electron reduced species of metal complexes resulted in formation of the two-electron reduced species from which H_2 is formed.[17] Bimolecular reactions of metal(III)-hydride complexes also generate H_2 accompanied by regeneration of metal(II) complexes.[18] In each case, the maximum quantum yield of H_2 production per photon is 50%, because two photons are required to produce two electrons. Thus there has so far been no example for one photon to generate one H_2 molecule.

We report herein photocatalytic H_2 evolution from ascorbic acid ($AscH_2$) with a cobalt(II) chlorin complex [Co^{II}(Ch)] (a chemical structure shown in Scheme 1)[19] in an aqueous acetonitrile solution (H_2O/MeCN), which proceeds via a one-photon two-electron process. The photocatalytic mechanism is clarified by nanosecond laser transient absorption spectra and by examining each step in the catalytic cycle independently.

Visible light irradiation of a deaerated (Ar-saturated) H_2O/MeCN solution (1:1 v/v) of [$Ru(bpy)_3$]$^{2+}$ (bpy = 2,2'-bipyridine) containing ascorbic acid ($AscH_2$) and ascorbate ($AscH^-$) (E_{ox} = 0.43 V $vs.$ SCE) as an electron donor and Co^{II}(Ch) (E_{red} = –0.96 V $vs.$ SCE) [Fig. S1 in the supplementary information (ESI) †] as a catalyst resulted in H_2 evolution (Fig. 1, black line). When the ratio of $AscH^-$ to $AscH_2$ was changed as fixed total concentrations of $AscH_2$ and $AscH^-$ ([$AscH_2$] + [$AscH^-$] = 1.1 M), the largest H_2 evolution activity was attained with $AscH^-$ (0.30 M) and $AscH_2$ (0.80 M) (Fig. S2 in ESI †). The smaller concentration of $AscH^-$ results in less efficient reductive quenching of the [$Ru(bpy)_3$]$^{2+}$* emission (* denotes the excited state). The quenching efficiency of [$Ru(bpy)_3$]$^{2+}$* (E_{red} = 0.77 V $vs.$ SCE in MeCN)[20] by $AscH^-$ (0.30 M) with $AscH_2$ (0.80 M) was determined to be 95% (Fig. S3 in ESI †). On the other hand, the smaller concentration of $AscH_2$ may retard H_2 production due to decreasing the acidity. When H_2O was replaced by D_2O, D_2 and HD
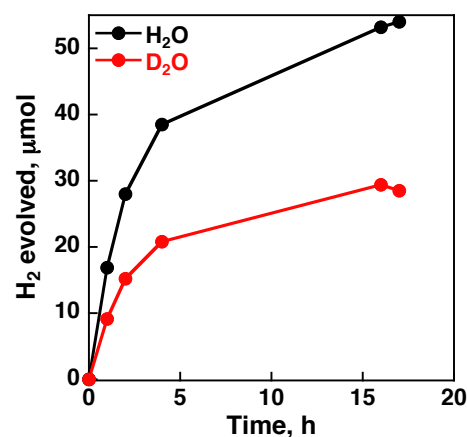
Fig. 1 Time courses of H_2 evolution in the photocatalytic reduction of proton in an Ar-saturated H_2O/MeCN (black) and D_2O/MeCN (red) mixed solution (1:1 v/v) containing [Ru^{II}(bpy)_3]$^{2+}$ (2.0 mM), $AscH_2$ (0.80 M), AscHNa (0.30 M) and Co^{II}(Ch) (25 μM) under irradiation of visible light (λ > 420 nm) at 298 K.

were produced without formation of H_2. Thus, hydrogen was produced from water and ascorbic acid as electron and proton sources. The observed deuterium kinetic isotope effect (KIE) in Fig. 1 ($k_H/k_D = 1.8$ in the initial stage) suggests that the Co-H bond cleavage of a cobalt hydride intermediate ($[Co^{III}(H)(Ch)]$) by proton may be the rate-determining step for the photocatalytic H_2 evolution (vide infra).

The concentration of $Co^{II}(Ch)$ was optimised to be 50 µM for the efficient photocatalytic H_2 evolution. The absorption of $[Ru(bpy)_3]^{2+}$ is blocked by the larger concentration of $Co^{II}(Ch)$ (Fig. S4 in ESI †).[21] The quantum yield of the photocatalytic H_2 evolution was determined to be 12% using a ferric oxalate actinometer (see the experimental section in ESI †). This value is similar to the highest value reported for photocatalytic H_2 evolution using a cobalt terpyridine complex ($\Phi = 0.13$).[22]
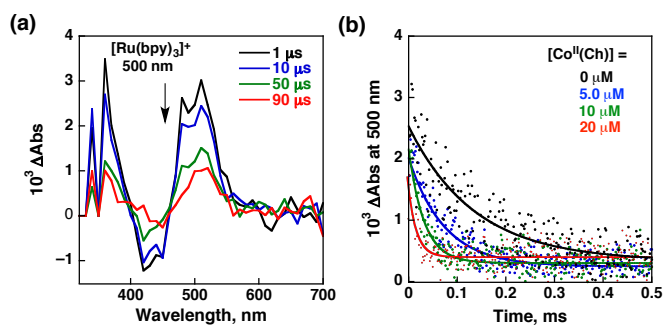
Fig. 2 (a) Transient absorption spectra after laser excitation ($\lambda = 450$ nm) of $[Ru^{II}(bpy)_3]^{2+}$ (80 µM) in the presence of $AscH_2$ (0.80 M) and AscHNa (0.30 M) in a deaerated H_2O/MeCN mixed solution (1:1 v/v) at 298 K. (b) Time profiles of absorbance at 500 nm due to decay of $[Ru(bpy)_3]^+$ in the presence of various concentrations of $Co^{II}(Ch)$ (0 – 20 µM) in deaerated H_2O/MeCN mixed solutions (1:1 v/v) containing $[Ru^{II}(bpy)_3]^{2+}$ (80 µM), $AscH_2$ (0.80 M), AscHNa (0.30 M).

Nanosecond transient absorption spectra of an H_2O/MeCN solution of $[Ru(bpy)_3]^{2+}$ with $AscH_2$ and $AscH^-$ are shown in Fig. 2, where appearance of the absorption band at 500 nm due to $[Ru(bpy)_3]^+$ is observed upon the nanosecond laser excitation. Thus, electron transfer from $AscH^-$ to $[Ru(bpy)_3]^{2+*}$ occurred to produce $AscH^{\bullet}$ and $[Ru(bpy)_3]^+$. The rate constant of electron transfer from $AscH^-$ to $[Ru(bpy)_3]^{2+*}$ (k_{et}) was determined to be 8.0×10^8 M^{-1} s^{-1} from a slope of Stern-Volmer plot ($K_{SV} = 3.5 \times 10^2$ M^{-1}) and the lifetime of $[Ru(bpy)_3]^{2+*}$ (0.44 µs in water/MeCN 1:1 v/v) (Fig. S5 in ESI †).[23] The decay rate of absorbance at 500 nm due to $[Ru(bpy)_3]^+$ obeyed the second-order kinetics of bimolecular back electron transfer from $[Ru(bpy)_3]^+$ to $AscH^{\bullet}$. In the presence of $Co^{II}(Ch)$, the decay of absorbance at 500 nm due to $[Ru(bpy)_3]^+$ became much faster because of electron transfer from $[Ru(bpy)_3]^+$ to $Co^{II}(Ch)$ as shown in Fig. 2b. The decay rate constant linearly increased with increasing the concentration of $[Co^{II}(Ch)]$ (Fig. S6 in ESI †). The rate constant of electron transfer from $[Ru(bpy)_3]^+$ to $Co^{II}(Ch)$ was determined to be 2.5×10^9 M^{-1} s^{-1} from the slope of dependence of the first-order decay rate constant on concentration of $Co^{II}(Ch)$ (Fig. S6b in ESI †).

To examine the reaction of $[Co^I(Ch)]^-$ that is produced by electron transfer from $[Ru(bpy)_3]^+$ to $Co^{II}(Ch)$, $[Co^I(Ch)]^-$ was prepared by the one-electron reduction of $Co^{II}(Ch)$ by decamethylcobaltocene $[Co(Cp^*)_2]$ in MeCN (Fig. S7 in ESI †). The UV-vis absorption band of $[Co^I(Ch)]^-$ (red line in Fig. 3a; $\lambda_{max} =$
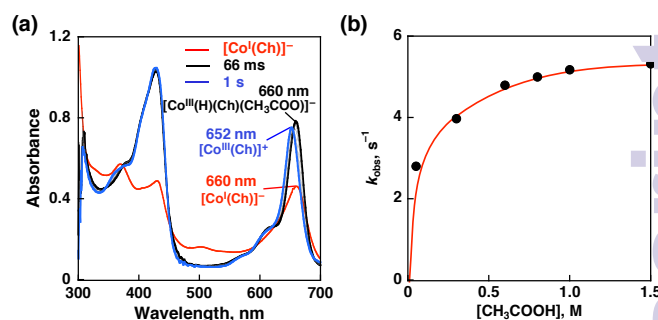

Fig. 3 (a) UV-vis absorption spectral changes of $[Co^I(Ch)]^-$ (30 µM) upon addition of CH_3COOH (0.30 M) in dearated MeCN at 298 K. The black and blue lines show the spectra taken at 66 ms and 1 s after mixing, respectively. The red line shows UV-vis absorption spectrum of $[Co^I(Ch)]^-$ (15 µM) formed by the electron-transfer reduction of $Co^{II}(Ch)$ (15 µM) with $CoCp^*_2$ (300 µM) in dearated MeCN at 298 K. (b) Plot of k_{obs} for the rate of formation of $[Co^{III}(Ch)]^+$ vs. $[CH_3COOH]$.

510 nm) decreased with increasing absorption band at 660 nm (black line) at 66 ms after addition of acetic acid (CH_3COOH) (0.30 M). Then, this absorption band was finally blue shifted $\lambda_{max} = 652$ nm, which is due to $[Co^{III}(Ch)]^+$.[24,25] Thus, $[Co^I(Ch)]^-$ may react with CH_3COOH to form the hydride complex ($[Co^{III}(H)(Ch)(CH_3COO)]^-$: $\lambda_{max} = 660$ nm), from which H_2 was evolved by the reaction with CH_3COOH to produce $[Co^{III}(Ch)]^+$. The reaction of $[Co^I(Ch)]^-$ with CH_3COOH was monitored by the absorption change at 652 nm due to $[Co^{III}(Ch)]^+$ as shown in Fig. 3, where the rate of the formation of $[Co^{III}(Ch)]^+$ obeyed first-order kinetics (Fig. S8 in ESI †). The first-order rate constant increased with increasing concentration of CH_3COOH to approach a constant value (Fig. 3b). Such a saturation behavior indicates that CH_3COOH is not involved in the rate-determining step and that the reaction of $[Co^I(Ch)]^-$ with CH_3COOH proceeds via formation of the hydride complex ($[Co^{III}(H)(Ch)(CH_3COO)]^-$), followed by the rate-determining heterolytic cleavage of the Co^{III}-H bond. The subsequent reaction of the released hydride ion with CH_3COOH to produce H_2 and $[Co^{III}(Ch)]^+$ may be fast as compared with the back reaction of the Co^{III}-H bond cleavage (Scheme 1). The kinetic equation for the formation of $[Co^{III}(Ch)]^+$ is given by eqn (1),

$$d[[Co^{III}(Ch)]^+]/dt = k[[Co^{III}(H)(Ch)(CH_3COO)]^-] \quad (1)$$
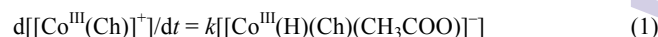
where k is the rate constant of the hydrogen evolution. From the equilibrium constant (K), the concentration of a complex between $[Co^I(Ch)]^-$ and CH_3COOH is given by eqn (2), where $[[Co^I(Ch)]^-]_0$
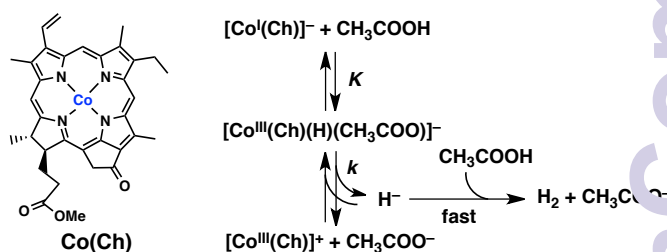
Scheme 1 Mechanism of hydrogen formation by the reaction of $[Co^I(Ch)]^-$ with CH_3COOH.

$$[[Co^{III}(H)(Ch)(CH_3COO)]^-]$$
$$= K[CH_3COOH]([[Co^I(Ch)]^-]_0 - [[Co^{III}(Ch)]^+])/(1 + K[CH_3COOH]) \quad (2)$$

is the initial concentration. Equation (1) is rewritten by eqn (3).

$$d[[Co^{III}(Ch)]^+]/dt = kK[CH_3COOH]([[Co^I(Ch)]^-]_0 - [[Co^{III}(Ch)]^+])$$
$$/(1 + K[CH_3COOH]) \quad (3)$$

Under the conditions, the concentration of CH_3COOH is much higher than that of $[Co^I(Ch)]^-$, the k_{obs} value is given by eqn (4). To determine the k value, eqn (4) is rewritten by eqn (5), which predicts

$$k_{obs} = kK[CH_3COOH]/(1 + K[CH_3COOH]) \quad (4)$$

$$k_{obs}^{-1} = 1/kK \cdot [CH_3COOH]^{-1} + 1/k \quad (5)$$

a linear correlation between k_{obs}^{-1} and $[CH_3COOH]^{-1}$ (Fig. S9 in ESI †). The k and K values were determined from the intercept and slope of the linear plot of k_{obs}^{-1} vs. $[CH_3COOH]^{-1}$ to be 5.9 s^{-1} and 7.1 M^{-1}.

When CH_3COOH was replaced by CH_3COOD, the deuterium kinetic isotope effect (KIE) was observed (Fig. S10 in ESI †),[26] indicating that the cleavage of the Co-H bond of $[Co^{III}(H)(Ch)(CH_3COO)]^-$ or O-H bond of CH_3COOH is involved in the rate-determining step of the reaction of $[Co^I(Ch)]^-$ with CH_3COOH. Because CH_3COOH is not involved in the rate-determining step (vide infra), the cleavage of the Co-H bond of $[Co^{III}(H)(Ch)(CH_3COO)]^-$ is the rate-determining step of the reaction of $[CoI(Ch)]^-$ with CH_3COOH. The KIE value was 1.7 which is virtually the same as observed for the photocatalytic H_2 evolution (KIE = 1.8, Fig. 1), indicating that the heterolytic Co-H bond cleavage of $[Co^{III}(H)(Ch)(CH_3COO)]^-$ is also the rate-determining step in the photocatalytic H_2 evolution.

$[Co^{III}(Ch)]^+$ produced by the reaction of $[Co^{III}(H)(Ch)-(CH_3COO)]^-$ with CH_3COOH is reduced by AscH$^-$ to produce $Co^{II}(Ch)$ as shown by stopped-flow measurements in Fig. 4.[27] The rate constant of electron transfer from AscH$^-$ to $[Co^{III}(Ch)]^+$ that was prepared by the one-electron oxidation of $Co^{II}(Ch)$ with (p-BrC$_6$H$_4$)$_3$N$^{•+}$SbCl$_6^-$ in $H_2O/MeCN$ was determined to be 1.5×10^3 M^{-1} s^{-1} from the linear dependence of the first-order rate constant on concentration of AscH$^-$ (Fig. S11 in ESI †).
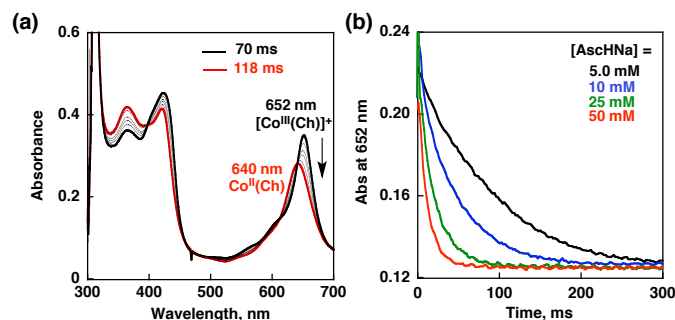
Fig. 4 (a) UV-vis absorption spectral changes in the electron-transfer reduction of $[Co^{III}(Ch)]^+$ (15 μM) with AscHNa (50 mM) in air-saturated $H_2O/MeCN$ mixed solutions (1:1 v/v) at 298 K taken at 70 ms and 118 ms after mixing. (b) Decay time profiles of absorbance at 652 nm due to $[Co^{III}(Ch)]^+$ in the presence of various concentrations of AscHNa in air-saturated $H_2O/MeCN$ mixed solutions (1:1 v/v) at 298 K.

The photocatalytic cycle is summarized in Scheme 2. Photoexcitation of $[Ru(bpy)_3]^{2+}$ resulted in electron transfer from AscH$^-$ to $[Ru(bpy)_3]^{2+*}$ to produce $[Ru(bpy)_3]^+$, followed by electron transfer from $[Ru(bpy)_3]^+$ to $Co^{II}(Ch)$ to produce $[Co^I(Ch)]^-$, which reacts with AscH$_2$ to produce $[Co^{III}(H)(Ch)(AscH)]^-$. Hydrogen is generated by the reaction of $[Co^{III}(H)(Ch)(AscH)]^-$ with AscH$_2$ via the Co-H bond heterolysis to produce $[Co^{III}(Ch)]^+$,[28,29] which is reduced by AscH$^-$ to regenerate $Co^{II}(Ch)$. In such a case, a one-photon two-electron process is made possible, because one photon is required to produce $[Co^I(Ch)]^-$ for H_2 evolution and another electron is provided thermally by AscH$^-$.
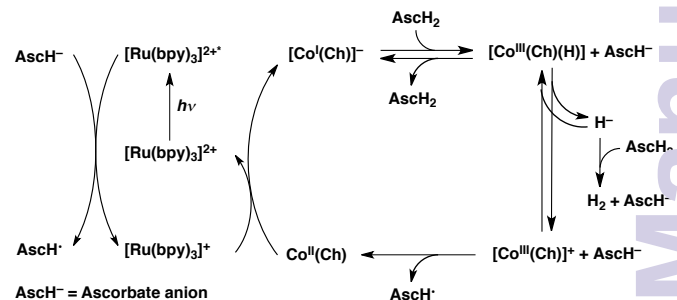
Scheme 2 Mechanism of photocatalytic hydrogen evolution from AscH$^-$ and AscH$_2$ with $[Ru(bpy)_3]^{2+}$ and $Co^{II}(Ch)$.

In conclusion, $Co^{II}(Ch)$ acts as an efficient catalyst for photocatalytic H_2 evolution from ascorbic acid with $[Ru(bpy)_3]^{2+}$ as a photocatalyst to attain the high quantum yield via a one-photon two-electron process in which the second electron is provided thermally from ascorbic acid.

Notes and references

^a *Department of Material and Life Science, Graduate School of Engineering, Osaka University, ALCA and SENTAN, Japan Science and Technology Agency (JST), Suita, Osaka 565-0871, Japan. E-mail: fukuzumi@chem.eng.osaka-u.ac.jp; Fax: +81-6-6879-7370*
^b *Department of Chemistry and Nano Science, Ewha Womans University, Seoul 120-750, Korea.*
^c *Faculty of Science and Technology, Meijo University, ALCA and SENTAN, Japan Science and Technology Agency (JST), Nagoya, Aichi 468-8502, Japan*

† Electronic Supplementary Information (ESI) available: Experimental details and cyclic voltammograms (Fig. S1), time courses of H_2 evolution (Fig. S2), Photoluminescence spectra (Fig. S3), UV-vis absorption spectra (Fig. S4) and kinetic data (Figs. S5-S11). See DOI: 10.1039/c000000x/

1   R. A. Kerr and R. F. Service, *Science*, 2005, **309**, 101.
2   X. Song, H. Wen, C. Ma, H. Chen and C. Chen, *New J. Chem*, 2015, **39**, 1734.
3   K. Kawano, K. Yamauchi and K. Sakai, *Chem. Commun.*, 2014, **50**, 9872.
4   X. Wang, S. Goeb, Z. Ji, N. A. Pogulaichenko and F. N. Castellano, *Inorg. Chem.*, 2011, **50**, 705.

5   L.-Z. Fu, L.-L. Zhou, L.-Z. Tang, Y.-X. Xhang and S.-Z. Zhan, *J. Power Sources*, 2015, **280**, 453

6   S. Fukuzumi, *Curr. Opin. Chem. Biol.*, 2015, **25**, 18

7   D. Basu, S. Mazumder, X. Shi, H. Baydoun, J. Niklas, O. Poluektov, H. B. Schlegel and C. N. Verani, *Angew. Chem., Int. Ed.*, 2015, **54**, 2105.

8   A. Call, Z. Codola, F. Acuna-Pares and J. Lloret-Fillol, *Chem. Eur. J.*, 2014, **20**, 6171.

9   H. Lv, W. Guo, K. Wu, Z. Chen, J. Bacsa, D. G. Musaev, Y. V. Geletii, S. M. Lauinger, T. Lian and C. L. Hill, *J. Am. Chem. Soc.*, 2014, **136**, 14015.

10 L. Chen, G. Chen, C.-F. Leung, S.-M. Yiu, C.-C. Ko, E. Anxolabéhère-Mallart, M. Robert and T.-C. Lau, *ACS Catal.*, 2015, **5**, 356.

11 A. Zarkadoulas, E. Koutsouri, C. Kefalidi and C. A. Mitsopoulou, *Coord. Chem. Rev.*, 2014, **11**, 6.

12 K. Maeda, M. Eguchi and T. Oshima, *Angew. Chem., Int. Ed.*, 2014, **53**, 13164.

13 J. Zhao, Y. Ding, J. Wei, X. Du, Y. Yu and R. Han, *Int. J. Hydrogen Energy*, 2014, **39**, 18908.

14 E. Deponti, A. Luisa, M. Natali, E. lengo and F. Scandola, *Dalton. Trans.*, 2014, **43**, 16345.

15 H. Ozawa and K. Sakai, *Chem. Commun.*, 2011, **47**, 2227.

16 A. Rodenberg, M. Orazietti, B. Probst, C. Bachmann, R. Alberto, K. K. Baldridge and P. Hamm, *Inorg. Chem.*, 2015, **54**, 646.

17 S. Fukuzumi, T. Kobayashi and T. Suenobu, *Angew. Chem., Int. Ed.*, 2011, **50**, 728.

18 J. L. Dempsey, B. S. Brunschwig, J. R. Winkler and H. B. Gray, *Acc. Chem. Res.*, 2009, **42**, 1995.

19 K. Mase, K. Ohkubo and S. Fukuzumi, *J. Am. Chem. Soc.*, 2013, **135**, 2800.

20 J. Yuasa and S. Fukuzumi, *J. Am. Chem. Soc.*, 2006, **128**, 14281.

21 The photocatalytic H_2 evolution in our optimized conditions, the absorption at $\lambda = 450$ nm of $[Ru(bpy)_3]^{2+}$ (2.0 mM, $\varepsilon_{450nm} = 1.4 \times 10^4$ M^{-1} cm^{-1}) is not significantly blocked by that of $Co^{II}(Ch)$ ($Abs_{450\ nm} = 0.38$; $\varepsilon_{450\ nm} = 1.8 \times 10^4$ M^{-1} cm^{-1}) under this experimental conditions.

22 C. V. Krishnan and N. Sutin, *J. Am. Chem. Soc.*, 1981, **103**, 2141.

23 The emission lifetime of $[Ru(bpy)_3]^{2+*}$ in water at 298 K was reported to be 0.58 μs; see: J. V. Houten and R. J. Watts, *J. Am. Chem. Soc.*, 1976, **98**, 4853.

24 The spectrum of $[Co^{III}(Ch)]^+$ obtained by the reaction $[Co^I(Ch)]^-$ with CH_3COOH was identical to that of $[Co^{III}(Ch)]^+$ prepared by the electron-transfer oxidation of $Co^{II}(Ch)$ by a one-electron oxidizing reagent of $(p\text{-}BrC_6H_4)_3N^{\bullet+}SbCl_6^-$ ($E_{red} = 1.05$ V *vs.* SCE).[19]

25 $[Co^{III}(Ch)]^+$ or $[Co^{III}(H)(Ch)]$ species is not re-reduced by large excess of $Co(Cp^*)_2$, under the present reaction conditions because $Co^{II}(Ch)$ with 20 molar equiv. of $Co(Cp^*)_2$ is necessary to quantitatively produce $[Co^I(Ch)]^-$ as shown in ESI Fig. S7. $Co(Cp^*)_2$ ($E^{+/0}_{1/2} = -1.47$ V *vs.* SCE) is unstable even in carefully degassed and dehydrated MeCN.

26 The KIE value was determined from the k_{obs} values at $[CH_3COOH] = [CH_3COOD] = 1.0$ M.

27 Neither oxidation of $[Co^{III}(Ch)]^+$ nor O_2 reduction was observed under the basic reaction conditions.

28 S. Mandal, S. Shikano, Y. Yamada, Y.-M. Lee, W. Nam, A. Llobet and S. Fukuzumi, *J. Am. Chem. Soc.*, 2013, **135**, 15294.

29 No Co(II)-H complex is involved in the heterolysis of the Co-H bond as reported in ref. 28.

TOC
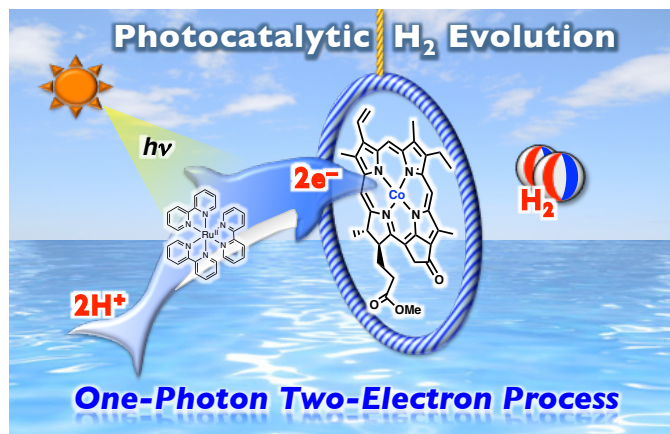
Text for TOC

A one-photon two-electron process was made possible in photocatalytic H$_2$ evolution from ascorbic acid with a cobalt(II) chlorin complex via electron transfer.